Chem. Mater. **2000,** *12,* 3906−3912

Synthesis of Nitrogen-Rich Carbon Nitride Networks from an Energetic Molecular Azide Precursor

Edward G. Gillan*

Department of Chemistry, University of Iowa, Iowa City, Iowa 52242-1294

Received July 13, 2000. Revised Manuscript Received October 19, 2000

Nitrogen-rich carbon nitrides are produced as amorphous, bulk solids from the slow thermal decomposition of 2,4,6-triazido-1,3,5-triazine [$(C_3N_3)(N_3)_3$]. This energetic molecular azide is thermally unstable and readily decomposes at 185 °C in a high-pressure reactor to produce carbon nitride materials, e.g., C_3N_4. Under applied nitrogen gas pressure, $(C_3N_3)(N_3)_3$ decomposes to yield a solid with one of the highest reported nitrogen-to-carbon ratios corresponding to C_3N_5. This azide precursor also decomposes upon rapid heating to 200 °C to form graphite nanoparticles without any retained nitrogen. Spectroscopic evidence (infrared, nuclear magnetic resonance, and ultraviolet−visible) demonstrates that the carbon−nitrogen solids have significant sp^2 carbon bonding in a conjugated doubly bonded network. Electron microscopy reveals that these powders have a glassy microstructure with large irregular pores and voids. C_3N_4 and C_3N_5 are thermally stable up to 600 °C and sublime to produce carbon nitride thin films on SiO_2 and Si substrates. A discussion on possible azide decomposition pathways and carbon nitride structures is presented.

Introduction

Carbon nitride (CN_x) materials have potential uses as hard coatings, battery electrodes, and catalyst supports, analogous to other Group 14 systems. Carbon-based solids with two- (sp^2) and three- (sp^3) dimensional bonding have utility as hard coatings,[1] electronic materials,[2] lithium intercalation electrodes,[3] catalytic supports,[4] and gas separation systems.[5] Recently, nanoscale graphitic particles and nanotubes were shown to incorporate and release molecular hydrogen.[6] While large nitrogen contents in silicon (Si_3N_4) and other Group 14 elements (e.g., Ge_3N_4 and Sn_3N_4)[7] are possible, analogous nitrogen-rich carbon nitrides are largely unknown. A theoretical treatment predicted diamondlike hardness for an sp^3-bonded carbon nitride phase (C_3N_4 or $CN_{1.33}$) with the β-Si_3N_4 structure[8] and spurred a considerable number of research efforts into CN_x synthesis over the past decade. In the intervening years much work on carbon nitrides has reached the literature, along with significant chemical and thermodynamic concerns about the stability of a β-C_3N_4 phase.[9,10]Other CN_x structures such as C_4N_3, cubic C_3N_4, and graphitic forms (C_3N_3, C_3N_4) has been discussed.[9−11] Much of the recent carbon nitride synthetic work utilizes elemental gas-phase processes such as laser ablation and radio frequency sputtering to produce thin films from about $CN_{0.2}$ to $CN_{1.0}$.[12]

Several reviews surveying CN_x materials suggest that β-C_3N_4 is kinetically stable at best, and synthesis via molecular precursor approaches offers a promising course of attack.[10b,13] One theoretical study examined precursors containing carbodiimide units ($-N{=}C{=}N-$) linked by sp^3 carbons or triazine (C_3N_3) rings and postulated that polymers derived from these precursors may convert to β-C_3N_4 under applied pressure.[14] Synthetic routes to bulk CN_x solids from molecular compounds usually require high temperatures (>700 °C) and result in nitrogen poor materials, e.g., $CN_{0.17}$ from C_5H_5N/Cl_2.[15] These syntheses are complicated by the facile formation of species such as $(CN)_2$ and HCN.

---

[1] For a recent review see *MRS Bull.* **1998**, *23* (9), 22−70.

[2] (a) Yakimova, R.; Janzen, E. *Diamond Relat. Mater.* **2000**, *9*, 432. (b) Spetz, A. L.; Tobias, P.; Baranzahi, A.; Martensson, P.; Lundstrom, I. *IEEE Trans. Electron. Dev.* **1999**, *46*, 561.

[3] Winter, M.; Besenhard, J. O.; Spahr, M. E.; Novak, P. *Adv. Mater.* **1998**, *10*, 725.

[4] (a) Gall, R. D.; Hill, C. L.; Walker, J. E. *Chem. Mater.* **1996**, *8*, 2523−2527. (b) Preiss, H.; Lischke, G.; Eckelt, R.; Miessner, H.; Meyer, K. *Carbon* **1994**, *32* (4), 587. (c) Park, C.; Baker, T. K. *J. Phys. Chem B.* **1998**, *102*, 5168.

[5] Armor, J. N. In *Materials Chemistry, An Emerging Discipline*; Interrante, L. V., Caspar, L. A., Ellis, A. B., Eds.; Advances in Chemistry Series; American Chemical Society: Washington, DC, 1995; Vol. 245, Chapt. 13.

[6] For a short review see Dresselhaus, M. S.; Williams, K. A.; Eklund, P. C. *MRS Bull.* **1999**, *24*, 45. (a) Chambers, A.; Park, C. Baker, T. K.; Rodriguez, N. M. *J. Phys. Chem. B* **1998**, *102*, 4253. (b) Chen, P.; Wu, X.; Lin, J.; Tan, K. L. *Science* **1999**, *285*, 91. (c) Liu, C.; Fan, Y. Y.; Cong, H. T.; Cheng, H. M.; Dresselhaus, M. S. *Science* **1999**, *286*, 1127.

[7] (a) Remy, J.-C.; Pauleau, Y. *Inorg. Chem.* **1976**, *15*, 2308. (b) Hoffman, D. M.; Rangarajan, S. P.; Athavale, S. D.; Economou, D. J.; Liu, J.-R.; Zheng, Z.; Chu, W.-K. *J. Vac. Sci. Technol. A* **1995**, *13*, 820, and references therein.

[8] (a) Liu, A. Y.; Cohen, M. L. *Phys. Rev. B* **1990**, *41*, 10727. (b) Cohen, M. L. *Mater. Sci. Eng. A* **1996**, *209*, 1.

[9] Hughbanks, T.; Tian, Y. *Solid State Commun.* **1995**, *96* (5), 321.

[10] (a) Badding, J. V.; Nesting, D. C. *Chem. Mater.* **1996**, *8*, 535. (b) Badding, J. V. *Adv. Mater.* **1997**, *9*, 877.

[11] (a) Teter, D. M.; Hemley, R. J. *Science* **1996**, *271*, 53. (b) Lowther, J. E. *Phys. Rev. B* **1999**, *59*, 11683. (c) Lowther, J. E. *Phys. Rev. B* **1998**, *57*, 5724.

[12] For a recent review see Muhl, S.; Mendez, J. *Diamond Relat. Mater.* **1999**, *8*, 1809. (a) Niu, C.; Lu, Y. Z.; Lieber, C. M. *Science* **1993**, *261*, 334. (b) Zhang, Z. J.; Huang, J.; Fan, S.; Lieber, C. M. *Mater. Sci. Eng. A* **1996**, *209*, 5. (c) Wu, M.-L.; Lin, X.-W.; Dravid, V. P.; Chung, Y.-W.; Wong, M.-S.; Sproul, W. D. *J. Vac. Sci. Technol A* **1997**, *15*, 946. (d) Yu, K. M.; Cohen, M. L.; Haller, E. E.; Hansen, W. L.; Liu, A. Y.; Wu, I. C. *Phys. Rev. B.* **1994**, *49*, 5034.

[13] Riedel, R. *Adv. Mater.* **1994**, *6*, 549.

[14] Kroll, P.; Hoffmann, R. *J. Am. Chem. Soc.* **1999**, *121*, 4696.

10.1021/cm000570y CCC: $19.00

Molecular precursor routes to CN_x include the high-pressure pyrolysis of tetracyanoethylene $[(CN)_2C{=}C(CN)_2]$ and triazine $[(C_3N_3)H_3]$,[16] shock compression of triazine-derived polymers,[17] and ambient pressure pyrolysis of multicyclic rings.[18] Generally these precursors result in compounds with 10−50 atom % nitrogen with the lowest incorporation at high reaction temperatures. The decomposition of molecules with triazine core structures such as $(C_3N_3)(NH_2)_3$ produces materials with substantial amounts of nitrogen[19] and sometimes significant residual hydrogen.[19a] Recently Kouvetakis et al.[20] demonstrated a creative chemical vapor deposition (CVD) process utilizing an organometallic triazine precursor, $[(R_3M)_2N](C_3N_3)Cl_2$, where R_3M is Me_3Si or Me_3Sn, in the synthesis of graphitic C_3N_4 films above 400 °C via R_3MCl elimination. Others recently investigated the CVD of the Me_3Si- precursor under a variety of conditions and found that hydrogen incorporation is sometimes a problem.[21]

In general, metallic or covalent nitrides are difficult to produce because stable molecules such as ammonia or N_2 are utilized as nitrogen sources. As a class of compounds, azides ($-N_3$) have been long recognized as ready sources of nitrogen and NaN_3 has found utility in a variety of metal nitride syntheses.[22] Azides are often unstable with respect to disproportionation; however, there are cases where a rapid degradation is desirable: for example, $Pb(N_3)_2$ was used as a primary explosive for many years,[23] and amine-stabilized $Ga(N_3)_3$ violently deflagrates to yield nanocrystalline GaN.[24] Azide-derivatized borazine (B_3N_3) rings were also recently converted to BN powders on careful heating.[25]

The title compound 2,4,6-triazido-1,3,5-triazine, $(C_3N_3)(N_3)_3$ or cyanuric triazide, is a moderately stable molecular azide. It was first synthesized[26] and structurally characterized[27] in the early part of this century and its structure was recently reexamined.[28] This molecule was briefly studied as an explosive and it is highly unstable with respect to disproportionation to C and N_2 ($\Delta H_f = +914$ kJ/mol).[29] Early vacuum work on this molecule demonstrated that it decomposed primarily to $(CN)_2$ and N_2 upon heating;[26] however, a recent study showed that $(C_3N_3)(N_3)_3$ detonates under pressure to produce graphite particles and a few percent carbon nanotubes.[30] There is also a report on vapor phase growth of $CN_{0.53}$ films from NCN_3 [one-third of the $(C_3N_3)(N_3)_3$ structure] and a nitrogen plasma.[31]

The molecular azide $(C_3N_3)(N_3)_3$ is unique as a carbon nitride precursor in that it contains *only* carbon−nitrogen or nitrogen−nitrogen bonds, no C−H, N−H, or cyanide species, and no other heteroatoms. This report demonstrates that *bulk* quantities of high nitrogen content CN_x material are produced from $(C_3N_3)(N_3)_3$ by retarding this azide's rapid deflagration process. This precursor's decomposition occurs at significantly lower temperatures than previous syntheses of bulk CN_x material and the resulting carbon nitrides have some of the highest reported C:N ratios, namely C_3N_4 and C_3N_5. These solids are thermally robust and sublime to a significant extent above 600 °C. The decomposition characteristics of the azide precursor and characterization of carbon nitride products are described below.

Experimental Section

$(C_3N_3)(N_3)_3$ Synthesis. The synthesis of 2,4,6-triazido-1,3,5-triazine [cyanuric triazide or $(C_3N_3)(N_3)_3$] was accomplished by minor modification of previous syntheses.[26] The reaction of $(C_3N_3)Cl_3$ (Aldrich, 99%) with a 10% excess of powdered NaN_3 (Aldrich, 99%) in refluxing reagent-grade acetone afforded a pale yellow $(C_3N_3)(N_3)_3$ product that was purified by recrystallization at −20 °C from distilled toluene. The resulting white, polycrystalline product is chemically stable under ambient atmospheric conditions; however, $(C_3N_3)(N_3)_3$ does exhibit shock sensitivity (e.g., it violently decomposes on rapid grinding in a mortar). **Warning: $(C_3N_3)(N_3)_3$ is a shock-sensitive and thermally unstable solid and should be treated with precautions afforded to similar potentially explosive materials.** The physical properties of the isolated material were in agreement with previous literature.[26−28] EI-MS *m/z* (ion, rel int): 204 ($M^+ = C_3N_{12}^+$, 30), 176 ($M^+ - 2N$, 1), 162 ($M^+ - 3N$, 1), 134 ($M^+ - 5N$, 1), 120 ($M^+ - 6N$, 2), 94 ($C_2N_5^+$, 12), 92 ($C_3N_4^+$, 10), 80 ($C_2N_4^+$, 5), 78 ($C_3N_3^+$, 8), 66 ($C_2N_3^+$, 100), 64 ($C_3N_2^+$, 60), 54 (CN_3^+, 35), 52 ($C_2N_2^+$, 40).

Thermal Decomposition Studies. Large-scale (ca. 0.5−1 g, 2.45−4.9 mmol) $(C_3N_3)(N_3)_3$ decomposition studies were performed in a 71 mL high-pressure, high-temperature stainless steel reactor (Parr, model 4740). An analog gauge on the reactor head monitored internal pressure and an external thermocouple measured the vessel temperature. $(C_3N_3)(N_3)_3$ was loaded into the reactor, which was evacuated and refilled with 1 atm of N_2 for ambient pressure reactions or 6 atm of N_2 for elevated pressure reactions. The reactor was heated in a vertical tube furnace (Thermolyne model 21100).

Carbon Nitride Sublimation. Acetone-cleaned Si (111) and SiO_2 wafers were sealed in a necked silica ampule with carbon nitride powder placed at the opposite end of the tube. The sealed evacuated ($P < 30$ mTorr) ampules were placed in a horizontal tube furnace with the wafers positioned near the exit of the furnace.

Precursor and Product Characterization. Solid electron impact mass spectrometry (EI-MS) was performed with a VG Trio1 system. $(C_3N_3)(N_3)_3$ volatilized easily so no external

---

(15) (a) Kouvetakis, J.; Kaner, R. B.; Sattler, M. L.; Bartlett, N. *J. Chem. Soc., Chem. Commun.* **1986**, 1758. (b) Kim, D.-P.; Lin, C. L.; Mihalisin, T.; Heiney, P.; Labes, M. M. *Chem. Mater.* **1991**, *3*, 686.

(16) Sekine, T.; Kanda, H.; Bando, Y.; Yokoyama, M.; Hojou, K. *J. Mater. Sci. Lett.* **1990**, *9*, 1376.

(17) (a) Wixom, M. R. *J. Am. Ceram. Soc.* **1990**, *73*, 1973. (b) Komatsu, T.; Samejima, M. *J. Mater. Chem.* **1998**, *8*, 193. (c) Komatsu, T. *J. Mater. Chem.* **1998**, *8*, 2475.

(18) For a review see Subrayan, R. P.; Rasmussen, P. *Trends Polym. Sci.* **1995**, *3* (5), 165. (a) Maya, L.; Cole, D. R.; Hagaman, E. W. *J. Am. Ceram. Soc.* **1991**, *74*, 1686. (b) Coad, E. C.; Kampf, J.; Rasmussen, P. G. *J. Org. Chem.* **1996**, *61*, 6666.

(19) (a) Montigaud, H.; Tanguy, B.; Demazeau, G.; Courjault, S.; Birot, M.; Dunogues, J. *C. R. Acad. Sci. Paris, Ser. 2* **1997**, *325*, 229. (b) Purdy, A. P.; Callahan, J. H. *Main Group Chem.* **1998**, *2*, 207.

(20) (a) Kouvetakis, J.; Bandari, A.; Todd, M.; Wilkens, B. *Chem. Mater.* **1994**, *6*, 811. (b) Todd, M.; Kouvetakis, J.; Groy, T. L.; Chandrasekhar, D.; Smith, D. J.; Deal, P. W. *Chem. Mater.* **1995**, *7*, 1422.

(21) Ivanov, B. L.; Zambov, L. M.; Georgiev, G. T.; Popov, C.; Plass, M. F.; Kulisch, W. *Chem. Vap. Deposition* **1999**, *5*, 265.

(22) (a) Gillan, E. G.; Kaner, R. B. *Inorg. Chem.* **1994**, *33*, 5693. (b) Yamane, H.; Shimada, M.; Clarke, S. J.; DiSalvo, F. J. *Chem. Mater.* **1997**, *9*, 413.

(23) *Energetic Materials: Physics and Chemistry of the Inorganic Azides*; Fair, H. D., Walker, R. F., Eds.; Plenum Press: New York, 1977.

(24) Frank, A. C.; Fischer, R. A. *Adv. Mater.* **1998**, *10*, 961.

(25) Paine, R. T.; Koestle, W.; Borek, T. T.; Wood, G. L.; Pruss, E.; Duesler, E. N.; Hiskey, M. A. *Inorg. Chem.* **1999**, *38*, 3738.

(26) Ott, E.; Ohse, E. *Ber. Dtsch. Chem. Ges.* **1921**, *54*, 179.

(27) (a) Hughes, E. W. *J. Chem. Phys.* **1935**, *3*, 1. (b) Knaggs, I. E. *Proc. R. Soc. (London)* **1935**, *A150*, 576.

(28) Kessenich, E.; Klapötke, T. M.; Nöth, H.; Schulz, A. *Eur. J. Inorg. Chem.* **1998**, 2013.

(29) Meyer, R. *Explosives*, 3rd ed.; VCH: New York, 1987; p 70.

(30) Kroke, E.; Schwarz, M.; Buschmann, V.; Miehe, G.; Fuess, H.; Riedel, R. *Adv. Mater.* **1999**, *11*, 158.

(31) Benard, D. J.; Linnen, C.; Harker, A.; Michels, H. H.; Addison, J. B.; Ondercin, R. *J. Phys. Chem. B* 1998, *102*, 6010−6019.

heating was necessary, and the sample was heated to ca. 250 °C by the electron impact process. Solution ^{13}C NMR was performed in C_6D_6 on a Bruker AC300 spectrometer. Solid-state ^{13}C NMR experiments were run on a Bruker MSL-300 system with a carbon Larmor frequency of 75.47 MHz and a conventional magic-angle spinning (MAS) arrangement and were referenced relative to an external hexamethylbenzene standard. Experiments were performed with a 7 mm Bruker CP/MAS probe and a spinning speed of 4 kHz. The free induction decays were recorded with a Hahn (90−180) echo sequence in order to eliminate distortions from probe ringing and background signals. Typical experimental parameters included a 5.75 μs 90° pulse, 50 kHz sweep width, 200 μs delay between the 90° and 180° pulse, and a recycle delay of 100 s. Infrared spectroscopy was performed on a Nicolet Nexus 670 spectrometer in transmission mode, either on KBr pellets or by direct transmission through Si wafers. UV−visible spectroscopic data were obtained from films on SiO_2 wafers with an HP 8453 diode array system. Thermogravimetric/differential thermal analysis (TG-DTA) was run on a Seiko Exstar 6300 system under argon or dilute oxygen flow. Bomb calorimetry was performed with a Parr oxygen calorimeter. Scanning electron microscopy (SEM) was executed with a Hitachi S-4000 field emission system on loose and lightly pressed samples. Transmission electron microscopy (TEM) was performed on methanol-dispersed powders on coated Cu grids by use of a Hitachi H-600 STEM system operating at 100 kV. X-ray diffraction (XRD) of powders and films was obtained with a Siemens D-5000 diffractometer. Density values were determined by a $CHCl_3/CHBr_3$ flotation method, which yielded a graphite density of 2.28 g/cm^3 (lit. value 2.26 g/cm^3). Bulk elemental analysis was obtained from Desert Analytics (www.desertanalytics.com). Modified CHN combustion under oxygen-free conditions was used for the oxygen determination.

Results

$(C_3N_3)(N_3)_3$ Synthesis and Stability. The $(C_3N_3)(N_3)_3$ precursor is conveniently produced in multigram batches via alkyl halide elimination in acetone with commercially available starting materials:

$$(C_3N_3)Cl_3 + 3\ NaN_3 \rightarrow (C_3N_3)(N_3)_3 + 3\ NaCl \tag{1}$$

The mass spectrum of $(C_3N_3)(N_3)_3$ shows successive nitrogen losses from the parent and evidence of $C_3N_6^+$ and $C_3N_4^+$ transients. A melting point capillary examination of this molecular azide showed the following characteristics: sharp melting to a clear liquid at 94−95 °C, gas evolution starting at 155 °C, orange to brown solution coloration by 170 °C, solidification to an orange-brown solid by 200 °C, and rapid decomposition at 240 °C.

Bomb calorimetry on $(C_3N_3)(N_3)_3$ under oxidizing and inert (argon) conditions showed energy releases of 2234 and 740 kJ/mol, respectively. The oxygen data correspond to a ΔH_f of +1053 kJ/mol, assuming CO_2 and N_2 are the only decomposition products, which is consistent with previous measurements.[29] It is interesting to note that the combustion enthalpy of $(C_3N_3)(N_3)_3$ is comparable to that of the military explosive RDX, $(C_3N_3)(NO_3)_3H_6$, which releases 2100 kJ/mol of energy; however, RDX is more thermodynamically stable ($\Delta H_f = +79$ kJ/mol).[29]

Simultaneous TG-DTA of $(C_3N_3)(N_3)_3$ under argon surprisingly showed that this energetic compound vaporizes completely after melting without detectable decomposition. When a loose platinum cover was placed over the solid to prevent complete volatilization, an exothermic event was observed by DTA near 225 °C (Figure 1).

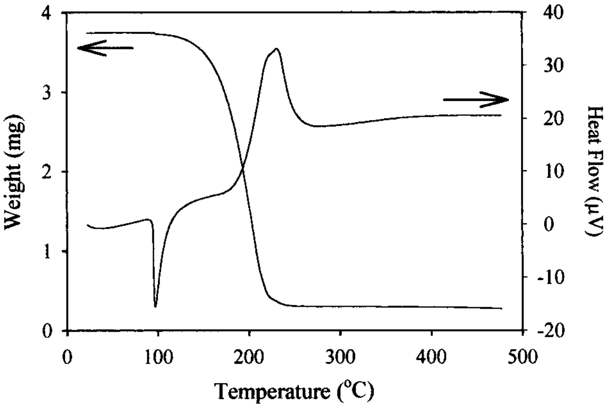

Figure 1. Thermal analysis (TG/DTA, argon flow, 5 °C/min) of partially covered $(C_3N_3)(N_3)_3$.

Table 1. Chemical Analysis and Density of Carbon Nitride Powders

sample reaction conditions	C, wt %	N, wt %	H, wt %	O, wt %	formulation $(C_3\mathbf{N}_x)\mathbf{H}_y\mathbf{O}_z$	density, g/cm^3
$(C_3N_3)(N_3)_3$, 185 °C decomp, 1 atm of N_2	38.0	57.5	1.53	3.08	$(C_3N_{3.9})H_{1.4}O_{0.2}$ $\approx C_3N_4$	1.60
$(C_3N_3)(N_3)_3$, 185 °C decomp, 6 atm of N_2	33.2	60.3	1.17	5.38	$(C_3N_{4.7})H_{1.3}O_{0.4}$ $\approx C_3N_5$	1.64
C_3N_5 sublimation residue (450 °C)	38.8	58.1	0.98	3.83	$(C_3N_{3.9})H_{0.9}O_{0.2}$ $\approx C_3N_4$	1.82
C_3N_5 sublimation residue (650 °C)	44.6	49.5	0.74	4.31	$(C_3N_{2.9})H_{0.6}O_{0.2}$ $\approx C_3N_3$	1.81

Decomposition Studies. In an attempt to isolate the orange-brown solid observed during the melting point determination, a steel reactor was loaded with $(C_3N_3)(N_3)_3$, evacuated, refilled with 1 atm of N_2, and slowly heated to 185 °C over 1 h. Gas evolution was slow and steady at 185 °C and reached a maximum pressure that corresponded to roughly 3 mol of gas per precursor molecule. The temperature was maintained for 2 days; however, no pressure increase was observed after 12 h. A free-flowing orange-brown powder [39% solids recovery based on $(C_3N_3)(N_3)_3$ used] was isolated from the reactor, washed with distilled toluene to remove any remaining precursor and soluble decomposition products, dried under dynamic vacuum, and stored in an argon-filled glovebox. When the above decomposition was performed in a reactor pressurized with 6 atm of N_2, the product consisted of brown, hard, brittle millimeter-sized pieces, which were isolated in the same manner described above. The bulk elemental analyses and flotation densities of both CN_x materials are listed in Table 1. The powder from ambient pressure decomposition is consistent with a C_3N_4 formulation, while the solid produced under applied pressure corresponds to nearly C_3N_5. The hydrogen residue in each sample is likely a consequence of tying up reactive bonds that may be present in the crude product; for example, unwashed C_3N_5 samples contain no hydrogen.[32] Over a period of months in air these CN_x samples become slightly lighter in color; however, reanalysis of C_3N_4 samples yielded essentially unchanged C, N, and H percentages. The color changes may correspond to coordination events, since recent studies have shown that CN_x materials

---

[32] Elemental analysis (wt %): C (34.45), N (61.78), H (<0.05), O (2.34).

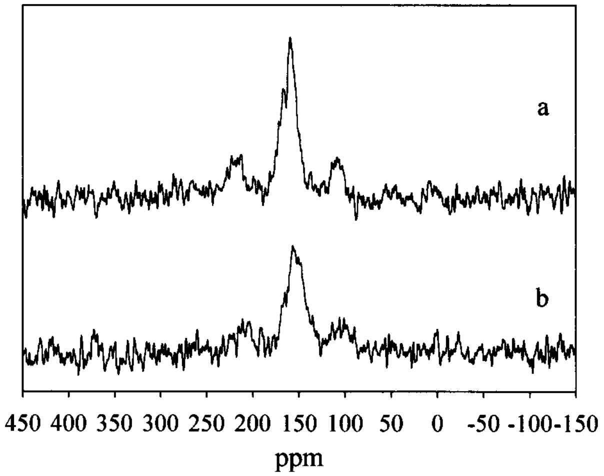

Figure 2. ^{13}C MAS NMR spectra of (a) C_3N_4 and (b) C_3N_5.

have a strong propensity to adsorb water.[31,33] Neither of these carbon nitrides showed detectable solubility or reactivity in conventional solvents including H_2O, ethanol, toluene, diethyl ether, and THF.

The above results contrast with the rapid decomposition of $(C_3N_3)(N_3)_3$ initiated by a heated filament (e.g., bomb calorimetry in argon) or rapid external heating in a high-pressure reactor. In the latter case, increasing the vessel temperature rapidly to 195−200 °C produced an audible pop and a large, rapid pressure jump that was over 40% higher than the 185 °C decomposition. A small amount of a black solid was recovered [ca. 10% solids recovery based on $(C_3N_3)(N_3)_3$ used] and was >98 atom % carbon with almost no detectable nitrogen[34] and a density of 2.04 g/cm^3. No condensables (77 K) were isolated from the gaseous byproduct, though gas-phase IR showed an absorption in the cyanide region. Powder XRD of the black solid exhibited only one broad peak (d = 3.4 Å) consistent with graphite. SEM analysis (Supporting Information) showed that the graphitic particles are rather small (ca. 50−100 nm) and some have roughly hexagonal shapes. These results agree qualitatively with the rapid deflagration results by Kroke et al.,[30] where $(C_3N_3)(N_3)_3$ was detonated between copper and brass plates.

NMR and IR Analysis of C_3N_4 and C_3N_5. Neither C_3N_4 nor C_3N_5 was crystalline by powder XRD, so solid-state ^{13}C MAS NMR was performed to gain information on the local coordination environment in these systems. Both C_3N_4 and C_3N_5 spectra exhibit one broad peak centered at 158 and 156 ppm, respectively, consistent with sp^2-bonded carbon (Figure 2). A shoulder on the downfield side of the main peak is possibly present in each case. The other peaks are spinning side bands and no other carbon signals were observed. The downfield shift from aromatic carbon systems, e.g., benzene at 128 ppm, is consistent with sp^2 carbon centers deshielded by nitrogen neighbors. A similar shift is seen in carbon adjacent to nitrogen in pyridine (150 ppm). For comparison, the solution ^{13}C NMR of $(C_3N_3)Cl_3$ and $(C_3N_3)(N_3)_3$ have resonances at 171.7 and 172.2 ppm, respectively.

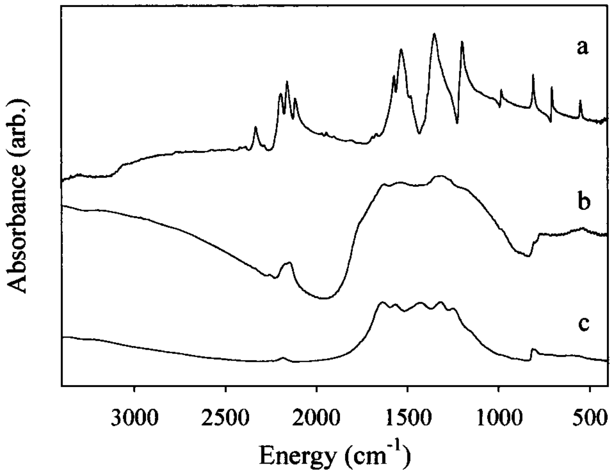

Figure 3. IR spectra of (a) the $(C_3N_3)(N_3)_3$ precursor and its low-temperature decomposition products (b) C_3N_5 and (c) C_3N_4.

Transmission IR spectra of C_3N_4, C_3N_5, and the parent $(C_3N_3)(N_3)_3$ are shown in Figure 3. The carbon nitride spectra are dominated by absorption events in the 950−1800 cm^{-1} region. This is also the dominant region of the precursor, indicating that these materials have structural features in common with $(C_3N_3)(N_3)_3$. The absorptions are consistent with conjugated C═N and C═C species (1600−1700 cm^{-1}), aromatic rings (1450−1600 cm^{-1}), N═N bonds (1440 cm^{-1}), aromatic C−N bonds (1270−1340 cm^{-1}), aliphatic C−N and secondary amines (1020−1250 cm^{-1}), and 1,3,5-substituted aromatic rings (810−950 cm^{-1}).[35] Notably, C_3N_4 and C_3N_5 show only minor absorption in the cumulated double bond (N═N═N or N═C═N) and triple bond (C≡N) region near 2200 cm^{-1}, in contrast to some previous reports on CN$_x$ materials that show significant absorption events in this region.[12b,17a,19b,36]

Electron Microscopy. SEM reveals that C_3N_4 and C_3N_5 have a smooth glassy morphology, in contrast to the particulate morphology of the graphitic carbon product. Figure 4a shows a smooth texture for C_3N_4 to below 100 nm. A similar structural morphology is demonstrated by C_3N_5 as shown in Figure 4b,c. The glassy features are interspersed with numerous irregular voids and pores and suggest a spongelike structure. TEM images of C_3N_5 show irregular particles and glassy surfaces (Supporting Information). Neither of these carbon nitride materials was crystalline by selected area electron diffraction.

Thermal Analysis and Vacuum Sublimation. Thermal analysis (TG-DTA) on C_3N_4 and C_3N_5 reveals that they are significantly robust and involatile up to 600 °C under an argon flow (Figure 5). The C_3N_5 product exhibits more stepwise losses at lower temperatures. Under a 20% oxygen flow these carbon nitrides fully oxidize by 550 °C. Since DTA under argon showed an endotherm near 600 °C for both compounds, the possibility of a CN$_x$ sublimation process was explored. Both C_3N_4 and C_3N_5 were sealed in evacuated silica ampules containing deposition substrates and placed in a tem-

---

[33] Zambov, L. M.; Popov, C.; Abedinov, N.; Plass, M. F.; Kulisch, W.; Gotszalk, T.; Grabiec, P.; Rangelow, I. W.; Kassing, R. *Adv. Mater.* **2000**, *12*, 656.

[34] Elemental analysis (wt %): C (97.92), N (0.04), H (<0.05).

[35] (a) Dean, J. A. *Lange's Handbook of Chemistry*, 14th ed.; McGraw-Hill: New York, 1992; Chapt. 7. (b) Silverstein, R. M.; Bassler, G. C.; Morrill, T. C. *Spectrometric Identification of Organic Compounds*, 5th ed.; John Wiley and Sons Inc.: New York, 1991.

[36] Li, D.; Chung, Y. W.; Yang, S.; Wong, M.-S.; Adibi, F.; Sproul, W. D. *J. Vac. Sci. Technol. A* **1994**, *12*, 1470.

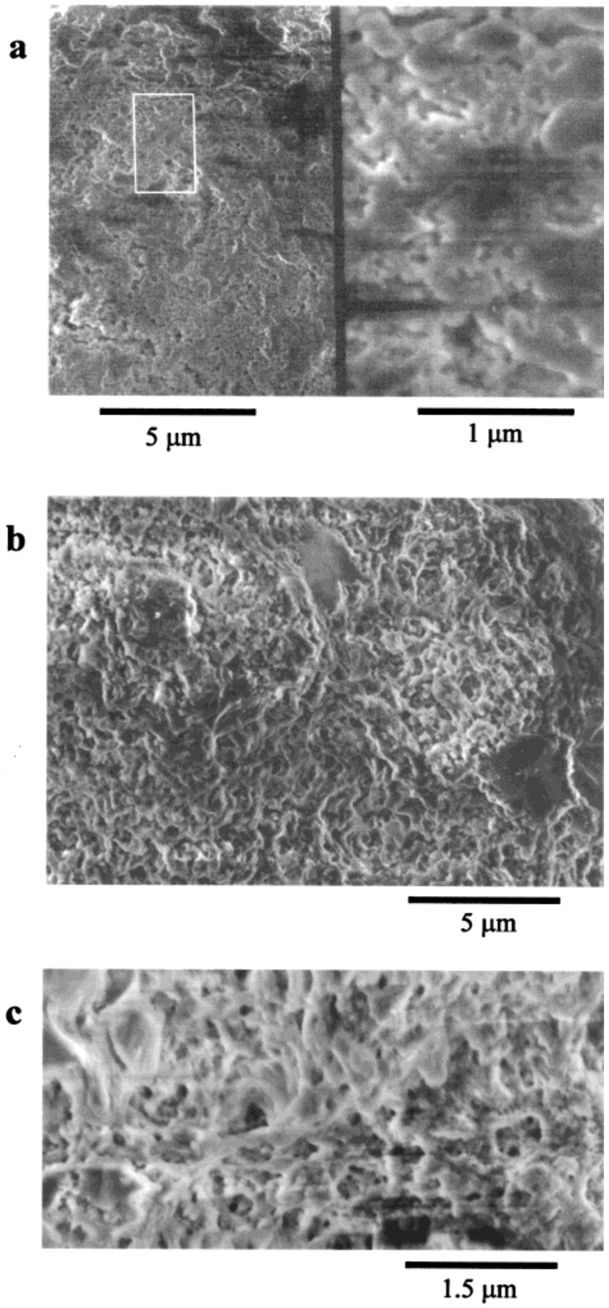

Figure 4. SEM analysis of (a) lightly pressed C_3N_4 powder (right frame is an expansion of boxed region in left frame) and (b, c) the surface of a C_3N_5 monolith.

perature gradient. Sublimation was slight at 450 °C and increased significantly by 650 °C. The film deposits were orange-yellow on SiO_2 and rainbow colored (interference fringes) on Si. The substrates were positioned near the exit of the furnace where most of the sublimed material redeposited. When the solid was heated to 650 °C, the deposition point was nearly 450 °C and the ampules still contained a vacuum after sublimation. Elemental analyses of the unsublimed C_3N_5 residue after 450 and 650 °C runs are listed in Table 1; there was a modest decrease in bulk nitrogen content as temperature increased. The sublimed films from C_3N_4 and C_3N_5 were still noncrystalline by powder XRD.

The transmission IR spectra of sublimed films and solid residues for C_3N_4 and C_3N_5 were very similar. Figure 6 compares as-synthesized C_3N_4 powder with a sublimed film on Si and the unsublimed residue remaining after heating at 650 °C. There is a striking similarity between C_3N_4 and its sublimation product; however, the 2180 cm^{-1} absorption is decreased in sublimed film and enhanced in the untransported solid relative to the C_3N_4 powder. Transmission UV−vis spectroscopy of the sublimed CN_x film on SiO_2 showed strong absorption in the 250−350 nm region consistent with nonbonding (N lone pairs) to π^* electronic transitions seen frequently in conjugated aromatic C=N systems.[35] Similar spectroscopic features are found in CVD-produced carbon nitride films grown from $(C_3N_3)(N_3)_3$ at 250 °C.[37]

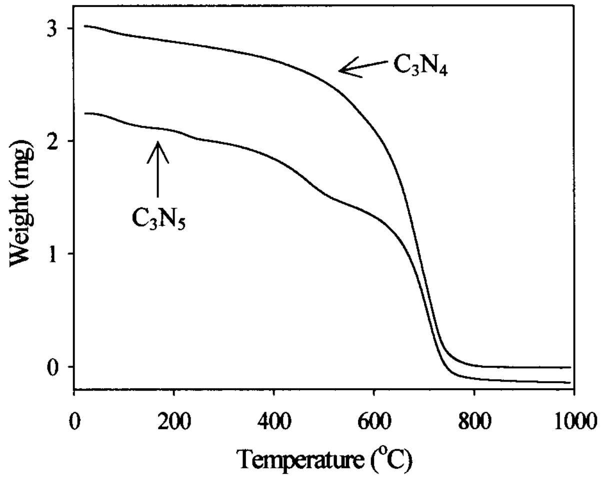

Figure 5. Thermal analysis (TGA, argon flow) of C_3N_4 and C_3N_5 powders. The C_3N_5 curve is offset for clarity.

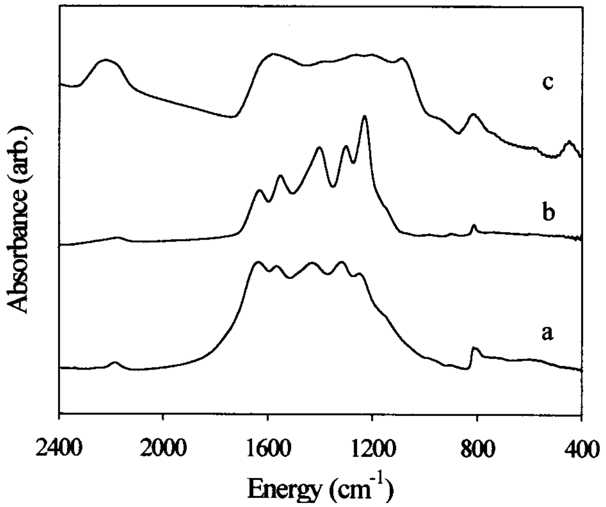

Figure 6. IR spectra for (a) as-synthesized C_3N_4 powder, (b) a sublimed CN_x film from C_3N_4 (650 to 450 °C gradient), and (c) the material remaining in the 650 °C zone.

Discussion

The search for viable synthetic routes to high nitrogen content CN_x materials is complicated by the thermodynamic instability of such compounds relative to graphite and nitrogen gas. For example, β-C_3N_4 has a calculated heat of formation ranging from +600 to +800 kJ/mol,[10] and other sp^2- and sp^3-bonded carbon nitrides have

---

(37) Wang, J.; Gillan, E. G. Unpublished results.

Scheme 1. Possible $(C_3N_3)(N_3)_3$ Decomposition Pathways

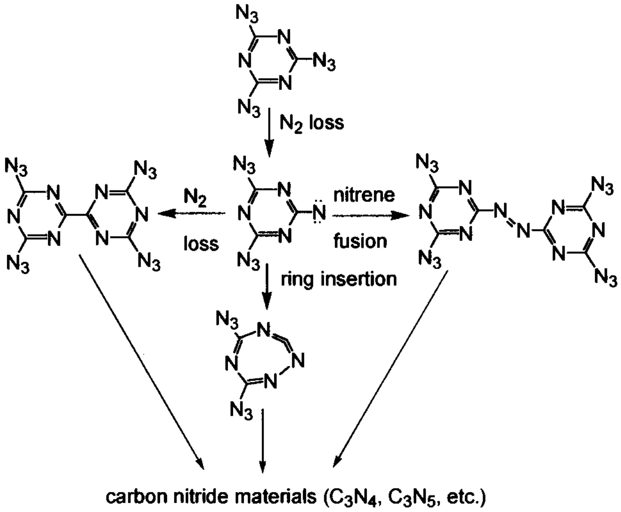

similarly large positive formation energies.[11] In the work reported above, the rapid decomposition (T > 200 °C) of an energetically unstable precursor, $(C_3N_3)(N_3)_3$, results in the thermodynamic end product, i.e., graphitic carbon nanoparticles and predominantly N_2 gas:

$$(C_3N_3)(N_3)_3 \rightarrow 3C\ (\text{graphite}) + 6N_2 \qquad (2)$$

The lower temperature decomposition of $(C_3N_3)(N_3)_3$ produces thermally robust carbon nitride materials with some of the highest bulk nitrogen contents reported to date, formulated as C_3N_4 and C_3N_5:

$$(C_3N_3)(N_3)_3 \rightarrow C_3N_{4+x} + [(8-x)/2]N_2 \qquad (3)$$

The $(C_3N_3)(N_3)_3$ precursor has an initial C:N ratio of 1:12 (80 atom % nitrogen) and favors the formation of nitrogen-rich phases. Pressurizing the reactor with excess nitrogen gas increases the nitrogen content of the final product and produces larger coherent masses.

Distinct modes for aromatic C−N species in IR and UV−vis spectra suggest that the triazine (sp^2) ring structure is largely intact in these carbon nitrides, and little absorption near 2000 cm^{-1} indicates that they do not contain appreciable cyanide or carbodiimide components. The solid-state ^{13}C NMR results also support an sp^2-type planar array of carbon and nitrogen. Graphitic C_3N_4 is predicted to exhibit a ^{13}C chemical shift of 144 ppm,[38] while amorphous sp^2-hybridized CN_x powders have reported shifts closer to 160 ppm.[36,39] The asymmetry in the ^{13}C peak for C_3N_4 and C_3N_5 suggests that carbon species are present with varying numbers of nitrogen neighbors, such as $N-C(N)_2$ versus $C-C(N)_2$. The downfield shifts are close to those of $(C_3N_3)(N_3)_3$, giving further credence to a nitrogen-rich carbon environment. The apparent porosity observed by SEM is consistent with the low densities (Table 1), which are similar to those of other amorphous CN_x films and powders.[19b,21] The voids observed by SEM are likely a consequence of nitrogen gas evolution during carbon nitride formation.

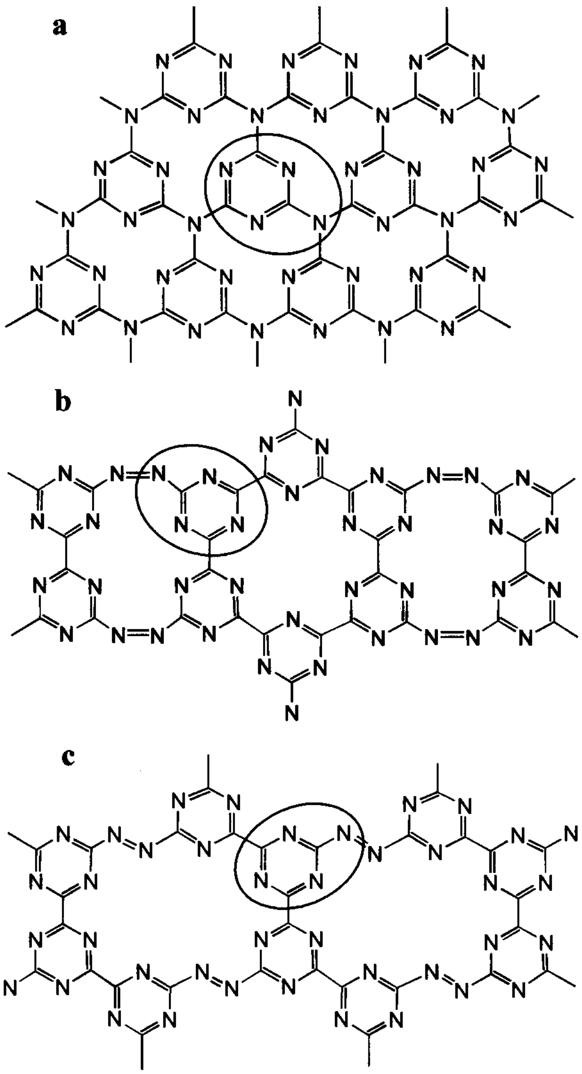

Figure 7. Idealized possible layered C_3N_4 structures resulting from triazine (C_3N_3) ring fusion after azide decomposition and N_2 loss: (a) remaining nitrenes bond to carbon atoms on other rings or (b, c) nitrenes form −N=N− bonds and rings form direct C−C bonds. One C_3N_4 unit is circled in each structure.

Previous studies on organic azide decomposition pathways provide useful insight on possible decomposition mechanisms operative in this work.[40] Recent photochemical studies at 10 K on an azidotriazine, $Cl_2(C_3N_3)N_3$, demonstrate that the azide decomposes via N_2 loss and produces a nitrene intermediate and nitrene ring insertion products.[41] These rearrangements have been proposed in various organic azide reactions.[42] The triazidotriazine used in the present study may decompose in a similar fashion; however, the degradation now occurs in neat liquid form at elevated temperatures so nitrene species on different rings may preferentially couple and form azobenzene-like connections (ring−N=

---

(38) Yoon, Y.-G.; Pfrommer, B. G.; Mauri, F.; Louie, S. G. *Phys. Rev. Lett.* **1998**, *80*, 3388.

(39) LaManna, J.; Braddock-Wilking, J.; Lin, S.-H.; Feldman, B. J. *Solid State Commun.* **1999**, *109*, 573.

(40) Nicolaides, A.; Tomioka, H.; Murata, S. *J. Am. Chem. Soc.* **1998**, *120*, 11530.

(41) Bucher, G.; Siegler, F.; Wolff, J. *J. Chem. Commun.* **1999**, 2113.

(42) (a) Smith, P. A. S. In *Azides and Nitrenes: Reactivity and Utility*; Scriven, E. F., Ed.; Academic Press: New York, 1984; Chapt. 3. (b) Benson, F. R. *The High Nitrogen Compounds*; John Wiley and Sons: New York, 1984; Chapt. 2.

N−ring).[43] A nitrene may also attack another ring or insert into its own triazine ring and produce cyclic carbodiimide species (Scheme 1).

Idealized structures of C_3N_4 planar products formed from intact C_3N_3 rings are shown in Figure 7. The first structure is based on a graphite sheet with regular holes, while the other structures are based on fused triazine rings in isolated six-ring units or infinite chains separated by −N═N− links. The high-pressure product, C_3N_5 may contain a larger number of −C−N═N−C− groups than C_3N_4 and have a greater tendency to thermally degrade under ambient pressure conditions.[42] It has been suggested that amorphous carbon nitrides with significant N−N bonding will lead to poorly interconnected networks.[11c] In the present work, the as-synthesized carbon nitride materials also appear to contain reactive bonds that are advantageously passivated by hydrogen during the toluene workup.

In *amorphous* sp^2-bonded carbon nitrides there is no limiting composition associated with a C_3N_4 formula, and extended structures with greater nitrogen contents are observed here. There is likely some degree of local bonding and compositional variation in these carbon nitrides produced via low-temperature $(C_3N_3)(N_3)_3$ decomposition; however, spectroscopically and thermally they appear reasonably homogeneous on a macroscopic level. On the basis of experimental evidence, it is reasonable to describe C_3N_4 and C_3N_5 as disordered planar systems somewhere between cross-linked polymers and graphitic sheets. The chemical reactivity, electrical properties, and photochemical stability of these carbon nitrides powders are currently under investigation. They may serve as a useful starting point in the synthesis of hard sp^3 carbon nitrides and composites or as intercalation materials and coordinatively active solid supports for metal complexes.

Acknowledgment. I gratefully acknowledge the assistance of Dr. Donald Stec and Jean Ross for solid-state NMR and TEM assistance, respectively. I also thank the Dreyfus Foundation for a New Faculty award and the Research Corporation for a Research Innovation Award.

Supporting Information Available: SEM photo of graphite nanoparticles and TEM photos of C_3N_5. This material is available free of charge via the Internet at http://pubs.acs.org.

CM000570Y

---

(43) Wilson, R. M.; Schnapp, K. A. *Chem. Rev.* **1993**, *93*, 223.